HETEROCYCLES, Vol. 75, No. 7, 2008, pp. 1711 - 1723. © The Japan Institute of Heterocyclic Chemistry
Received, 8th February, 2008, Accepted, 11th March, 2008, Published online, 14th March, 2008. COM-08-11361

RING CURRENT MODELS OF PORPHYRIN AND CONFORMATIONAL ANALYSIS OF THE DICARBOXYLATE COMPLEX OF Sn^{IV} PORPHYRIN

Hajime Iwamoto* and Yoshimasa Fukazawa*

Department of Chemistry, Graduate School of Science, Hiroshima University,
1-3-1 Kagamiyama, Higashi-Hiroshima 739-8526, Japan
E-mail: hiwamoto@hiroshima-u.ac.jp.

Abstract – Several models for the porphyrin ring current effect are constructed based on a classical line current approximation and their performances in reproducing the observed induced shifts of ligand protons in Sn^{IV}(porphyrin) dicarboxylate complexes are compared. A new model is selected and it is found that the diamagnetic ring current running on the inner 16π-electron circuit of the porphyrin is the main contributor together with a minor paratropic ring current on the outer 20π-electron circuit. Conformational analyses of bis(biphenyl carboxylate) complexes of Sn^{IV}(tetraphenylporphyrin) in solution were carried out with this porphyrin ring current effect model.

INTRODUCTION

Synthetic porphyrins and their metallo-derivatives have received considerable attention in many fields of chemistry.[1-4] Knowledge of the structures of porphyrins and their metallo-derivatives is essential to understand their structure function relationships. Although X-ray crystallographic analysis is one of the most frequently used structure elucidation methods, it provides only a limited number of structures in the solid state, and the structures obtained by this method do not always correspond with conformations that are significantly populated in solution.[5] Identification of the most populated structure of a metalloporphyrin complex in solution is not an easy task. It is well known that NMR chemical shifts reflect molecular structure. Variation in the local environment affects chemical shieldings, and the change in chemical shifts of nuclei caused by adjacent substituents provides valuable information about the relative arrangement of the nuclei under study with respect to these nearby substituents. The chemical shift changes caused by aromatic ring currents have thus been utilized for the conformational analysis of flexible compounds.[5-12] The ring current effect of porphyrin derivatives is also very important for the structure elucidation and conformational analysis of metalloporphyrin complexes in solution.[13] Many models of the porphyrin ring current effect have been reported[14-34] since the first report of the NMR spectra of porphyrins by Becker and Bradley.[35, 36]

We have previously developed a simple model of porphyrin ring current effects and used it successfully in the conformational analysis of bis(naphthalene-carboxylate) complexes of Sn^{IV}(porphyrin).[37-39] In our continuing studies, we have constructed several ring current models of porphyrin and compared the reproducibility in each model for the observed values of the porphyrin-induced chemical shift changes of several dicarboxylate complexes of Sn^{IV}(porphyrin). Here we report a new improved model for the porphyrin ring current effect and report the application of the new model to the conformational analyses of two dicarboxylate complexes of Sn^{IV}(tetraphenylporphyrin).

RESULTS AND DISCUSSION

Ring current models of porphyrins

Our previous model of the porphyrin ring current effect basically applies the classical line current approximation, as discussed originally by Salem.[40] In our simple model, the secondary magnetic field at a given proton is calculated on the assumption that electric currents flow exactly through C–C and C–N bonds of the porphyrin ring. The field (H') due to the current flowing in a polygon is the sum of contributions from the edges. The magnitude of the contribution of a particular edge AB at a point P is

$$H'_{AB} = J(\sin\theta_2 - \sin\theta_1)/\mathrm{cR}$$

where J is the line current and c is the speed of light (Figure 1). We employed this line current approximation to construct several ring current models of porphyrins (Figure 2). In model I, an electric current flows on two C–C bonds passing through a *meso* position and flows only on the inner arcs of all the pyrrole rings. In this model, the current runs on the inner circle of the porphyrin ring. In model II, a current on two C–C bonds runs only on the outer arcs of the pyrrole rings. Thus, in this model, the current runs on the outermost periphery of the porphyrin ring. The third model (III) is a hybrid of two 18π-electron systems, in one of which a current on two C–C bonds runs on the outer arcs of the pyrrole rings and then on the inner arcs of the following pyrrole alternately to reach the initial point. Both models IV and V are hybrids of models I and II. Model IV is a hybrid of two cooperative current loops of inner and outer π-electron systems. This model is the same as that reported previously.[37-39] Model V is a hybrid of two current loops in opposite flowing directions.

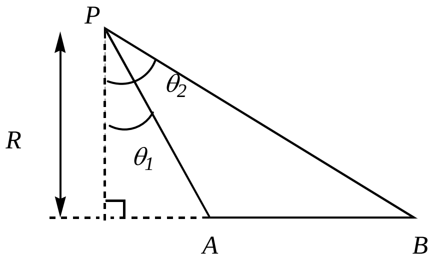

Figure 1. Calculation of magnetic field at P due to current in AB

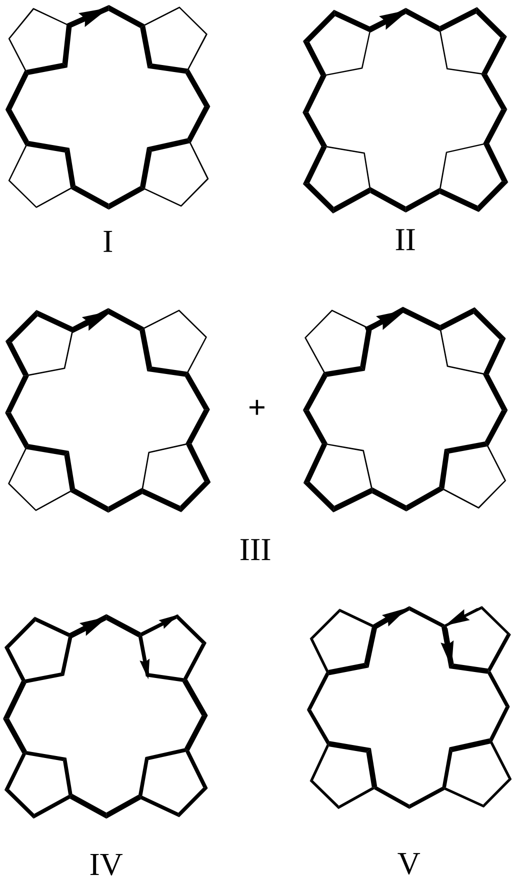

Figure 2. Ring current models

Structures of dibenzoate complexes of Sn^{IV}(porphyrin)

To construct models of the porphyrin ring current effect, the established geometry of those compounds having known induced shift values caused by the porphyrin ring current effect is necessary. For this reason, we employed four compounds (**1–4**) used in the previous current model[37-39] to estimate the magnitudes of the line currents of the outer and inner loops, respectively (Figure 3). In order to test the ring current models, six new complexes were prepared using 4-methylbenzoic acid, 3,5-dimethylbenzoic acid, and 3,5-di-*tert*-butylbenzoic acid as the new axial ligands for Sn^{IV}(tetraphenylporphyrin) (Sn^{IV}(tpp)) and Sn^{IV}(octaethylporphyrin) (Sn^{IV}(oep)). The observed chemical shift changes of these ligands in the complexes (**5–10**) are shown in Table 1 together with those of **1–4**.

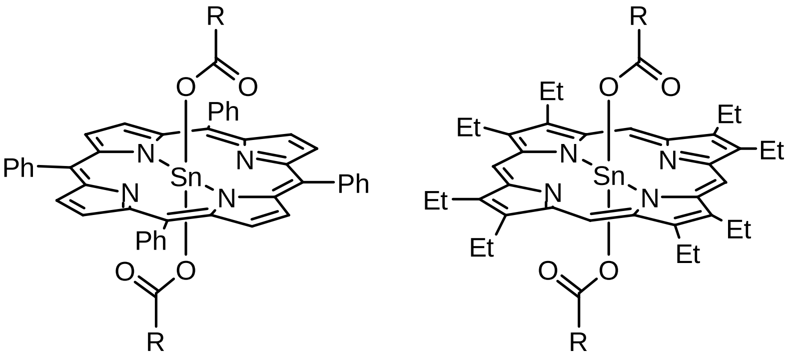

1 : R = Ph
3 : R = 1-adamantyl
5 : R = 3,5-dimethylphenyl
7 : R = 3,5-di-*tert*-butylphenyl
9 : R = 4-methylphenyl

2 : R = Ph
4 : R = 1-adamantyl
6 : R = 3,5-dimethylphenyl
8 : R = 3,5-di-*tert*-butylphenyl
10: R = 4-methylphenyl

Figure 3. Dicarboxylate complexes of $\mathrm{Sn^{IV}}$ porphyrin

Density functional theory (DFT) calculations (at the B3LYP/LANL2DZ level of theory) were carried out to obtain precise geometries of the new dicarboxylate $\mathrm{Sn^{IV}}$(porphyrin) complexes.[41] The calculated structures of **5** and **6** are shown in Figure 4.

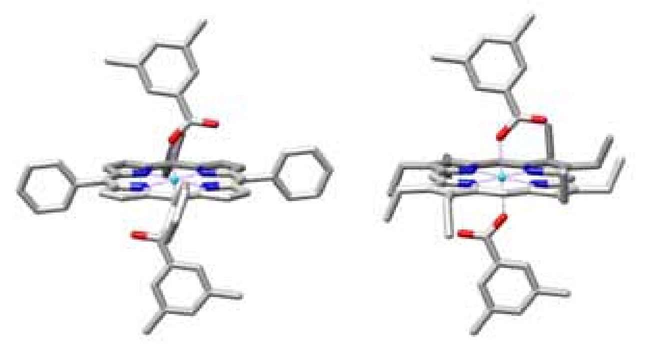

Figure 4. Molecular structures of **5** (left) and **6** (right) obtained from DFT calculations

In **5**, the benzene plane of the ligand in the calculated structure is perpendicular to the porphyrin plane. The carboxylate plane, which is almost identical to that of the benzene is roughly eclipsed with respect to the line connecting the two *meso* carbons on the porphyrin ring. The Sn–O bond is roughly perpendicular to the porphyrin plane. Since the C–C bond connecting the phenyl and carboxylate groups is not parallel to the Sn–O bond, the two *ortho* aromatic protons of the benzoate are not equidistant from the porphyrin plane. One peripheral phenyl ring on the porphyrin, which is the closest to the carbonyl oxygen of the benzoate, bends upward to a detectable extent. The diagonal phenyl ring on the porphyrin bends downward to achieve close proximity to the corresponding carbonyl oxygen of the *trans* benzoate. By contrast, the two proximal phenyl rings are neither bent upward nor downward.

In **6**, the structural characteristics found in **5**, except the upward bending of the peripheral substituent, are also seen in the calculated structure of the dibenzoate complex of $\mathrm{Sn^{IV}}$(oep) **6** (Figure 4). A similar perpendicular arrangement of the benzene plane with respect to the porphyrin ring was obtained. The carboxylate plane, which is nearly identical to that of the benzene, is again roughly eclipsed with respect to the line connecting the two *meso* carbons on the porphyrin ring.

The calculated structures of **7–10** are almost identical to the corresponding complexes (**5** and **6**) except for the substituents on the benzene ring of the axial ligands.

Evaluation of models of the ring current effect

The chemical shift differences between the free ligand and its metalloporphyrin complex are mainly caused by two factors: complexation shift and ring current effect. It is known that the complexation shifts are negligible at points other than close to the site of complexation.[42] In our complexes, all the protons are more than five bonds apart from the electropositive metal atom. Hence, we can safely assume that we do not need to consider the effect of the complexation shift on all the protons. We have obtained the structures of the complexes and the corresponding observed induced shift values of the ligands caused by the porphyrin ring current effect; accordingly, we can estimate the magnitude of the line current of the porphyrin ring by simple or multiple linear regression analysis based on the least-squares method. The coefficient of determination (R^2) in a linear regression analysis [32 data points (range of the observed up-field shifts 0.600–3.55 ppm)] between the observed and calculated induced shift values of the ligands is dependent on the magnitude of the current in each model. The magnitude of the current was determined so as to have the maximum value of the correlation coefficient with the regression analysis in each model. The root mean square (rms) error of the induced shift values of the ligands is also employed for this judgment. The best calculated values in each model are summarized in Table 1.

Satisfactory reproduction of the observed induced shift values of these complexes was given with model I (R^2 = 0.9963, rms = 0.0656 ppm). The best value of the correlation coefficient for model II is smaller than that for model I. The values of the correlation coefficients of models III and IV are between those of models I and II. These analyses indicate that the current loop running on the inner circuit of the porphyrin ring plays an important role in the estimation of the induced shift values of the ligands in these Sn^{IV}(porphyrin) complexes. Model V is a hybrid of models I and II. A least-squares fitting of the extent of contribution of the two models gave a small improvement ([$\Delta\delta_{obs.} = a \bullet \Delta\delta_{calc.}$; a = 0.9999, R^2 = 0.9964, rms = 0.0648 ppm] over model I in the rms value. In the new model, the magnitudes of the inner and outer currents are $1.886i_B$ and $-0.189i_B$, respectively where i_B is the magnitude of the line current of the benzene ring.[43] In this fitting, it is found that the current loop running on the inner circuit is the main contributor and that on the outer circuit is the minor. The signs of the two contributors are opposite to each other. This means that the directions of the two currents are opposite. In this model, it can also be said that the main inner current is perturbed by four local current loops of the four pyrrole rings. Thus, this fits with model V.

Both ring current models I and V gave satisfactory results. In these models, the inner circuit plays an important role in reproduction of the observed ring current induced shift values of the ligands. Apparently, the observed ligand protons are shielded when compared with their free ligands. This suggests that the effect of the porphyrin ring current is diatropic. As can be seen, however, the inner circuit is a 16π-electron system. It is well known that $4n$-membered π-electron circuits sustain paratropic currents.[44-46] Thus, it seems to be puzzling that the observed ring current due to the inner circuit is diatropic. This issue can be resolved when we consider the contribution of all the circuit currents of the porphyrin skeleton as has reported by Aihara for the circuit currents of polycyclic aromatic hydrocarbons.[47] The circuits that can be chosen from the porphyrin π-system are presented in Figure 5. The circuit currents formally obey Hückel's rule; $(4n + 2)$- and $4n$-membered circuits sustain diatropic and paratropic currents, respectively.[44-46] In these circuits, p1 and p4 are paratropic because they are 16- and 20-membered π-electron systems; both p2 and p3 are diatropic due to their 18-membered π-electron systems. The ring current effect of the porphyrin should be governed by the extent of the contribution of each circuit current. We cannot experimentally determine the extent of the contribution of the individual circuit currents; however, the diatropic ring current model I can be reasonably constructed if we assume that the magnitude of the p4 current is identical to that of the p2 (and p3). In this situation, the current through the outer arcs of the pyrrole rings can be cancelled out because the directions of currents p4 and p2 (p3) are opposite to each other because they are paratropic and diatropic, respectively. Although we don't know the extent of the contribution of the inner 16π-electron circuit (p1), the result of the contribution of the four circuits gives the net diatropic ring current of the 16π-inner circuit of model I. In the same sense, the ring current model V can be constructed using a slightly larger magnitude of the p4 current over that of the diatropic p2 (p3) current.

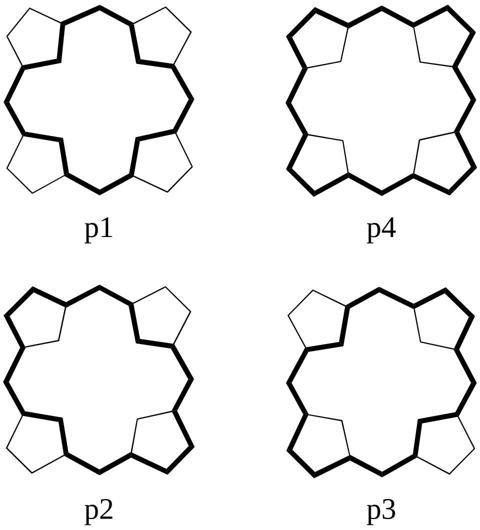

p1 p4

p2 p3

Figure 5. Circuits in porphyrin

Table 1. Observed and calculated chemical shift changes of ligand protons in dicarboxylate complexes of Sn^{IV}(porphyrin) (**1**–**10**, ppm) together with coefficients of determination R^2 and rms errors (ppm)

Nucleus	Shifts					
	Obs.	Calc.(I)	Calc.(II)	Calc.(III)	Calc.(IV)	Calc.(V)
H_o(**1**)	3.19	3.168	3.093	3.127	3.114	3.178
H_m(**1**)	1.15	1.144	1.222	1.189	1.202	1.133
H_p(**1**)	0.95	0.892	0.954	0.927	0.938	0.884
H_o(**2**)	3.53	3.467	3.390	3.425	3.411	3.477
H_m(**2**)	1.29	1.267	1.350	1.314	1.328	1.256
H_p(**2**)	1.07	0.981	1.046	1.018	1.029	0.972
2-H(**3**)	2.96	2.935	2.953	2.947	2.949	2.932
3-H(**3**)	1.10	1.147	1.249	1.205	1.223	1.133
4_{eq}-H(**3**)	1.17	1.211	1.299	1.261	1.276	1.198
4_{ax}-H(**3**)	0.81	0.881	0.950	0.920	0.932	0.871
2-H(**4**)	3.22	3.267	3.284	3.278	3.281	3.265
3-H(**4**)	1.22	1.277	1.377	1.334	1.351	1.263
4_{eq}-H(**4**)	1.26	1.373	1.469	1.428	1.444	1.359
4_{ax}-H(**4**)	0.92	0.993	1.064	1.033	1.045	0.983
H_o(**5**)	3.258	3.179	3.103	3.137	3.124	3.189
H_p(**5**)	0.934	0.898	0.959	0.933	0.943	0.889
Me(**5**)	0.777	0.824	0.914	0.876	0.891	0.812
H_o(**6**)	3.492	3.474	3.391	3.428	3.414	3.484
H_p(**6**)	1.063	0.987	1.050	1.023	1.034	0.978
Me(**6**)	0.868	0.927	1.019	0.979	0.995	0.915
H_o(**7**)	3.169	3.231	3.152	3.187	3.173	3.241
H_p(**7**)	0.995	0.902	0.964	0.938	0.948	0.894
Me(**7**)	0.685	0.693	0.798	0.753	0.771	0.679
H_o(**8**)	3.359	3.506	3.419	3.458	3.443	3.517
H_p(**8**)	1.137	0.992	1.056	1.029	1.039	0.983
Me(**8**)	0.752	0.781	0.886	0.841	0.859	0.767
H_o(**9**)	3.195	3.165	3.094	3.126	3.113	3.174
H_m(**9**)	1.144	1.148	1.227	1.193	1.206	1.137
Me(**9**)	0.600	0.661	0.720	0.695	0.705	0.653
H_o(**10**)	3.525	3.455	3.375	3.411	3.397	3.465
H_m(**10**)	1.277	1.267	1.348	1.314	1.327	1.256
Me(**10**)	0.664	0.725	0.786	0.760	0.770	0.716
R^2		0.9963	0.9898	0.9939	0.9925	0.9964
rms		0.0656	0.1093	0.0846	0.0937	0.0648

Conformational analysis of the biphenyl-carboxylate complex of Sn^{IV} (tetraphenylporphyrin)

Using the new set of parameters for the porphyrin ring current of the diatropic model V, conformational analyses of the di(4-phenylbenzoate) complex of Sn^{IV}(tpp) **11** and the di(3-phenylbenzoate) complex of Sn^{IV}(tpp) **12** in solution were carried out (Figure 6).

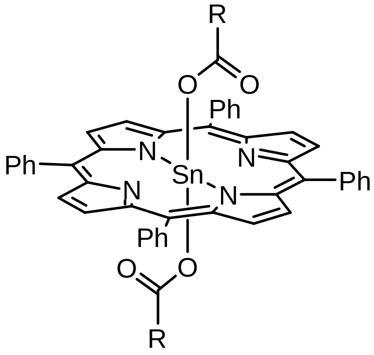

11 : R = 4-phenylphenyl
12 : R = 3-phenylphenyl

Figure 6. Dicarboxylate complexes of Sn^{IV}(porphyrin)

DFT calculations of **11** gave a twisted conformation of the biphenyl unit with a torsion angle of 45°, which suggests that the twisted form is more favorable than the planar biphenyl (Figure 7).

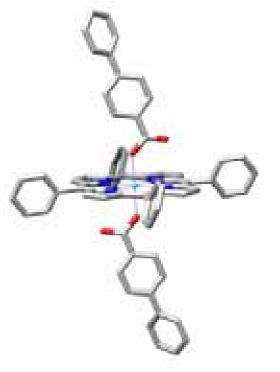

Figure 7. Molecular structure of **11** obtained from DFT calculations

With this DFT structure, the calculated ring current induced shift values of the ligand protons were estimated. Excellent correlation of these data was given in a linear regression analysis [five data points (range of the observed shift, 0.210–3.203 ppm) $\Delta\delta_{obs.} = a \bullet \Delta\delta_{calc.}$; a = 0.9983, R^2 = 0.9993], with satisfactorily small rms error (0.057 ppm) by using the new ring current model (Table 2).

Table 2. Observed (25 °C) and calculated ring current shifts of **11** (ppm)

Nucleus	Shifts	
	Obs.	Calc.
H_o	3.203	3.180
H_m	1.134	1.135
H_o	0.526	0.634
H_m	0.293	0.325
H_p	0.210	0.264

In the case of **12**, the situation is not so simple because there are two possible positions on the parent benzoate complex for the attachment of a phenyl ring to give the 3-phenylbenzoate complex. The two structures for **12**, *exo* and *endo* forms, were obtained with the DFT calculations (Figure 8). The calculated induced shifts of the aromatic protons of the two DFT structures were estimated (Table 3).

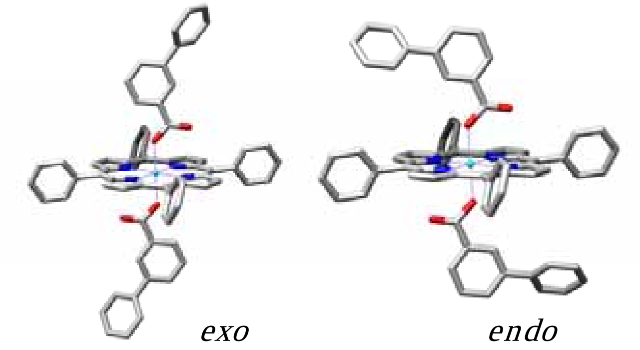

Figure 8. Molecular structures (exo, endo) of **12** obtained from DFT calculations

Table 3. Calculated ring current shifts of exo and endo conformers of **12** (ppm)

Nucleus	Shifts	
	exo	*endo*
H_2	1.888	4.436
H_4	0.892	0.885
H_5	1.328	0.968
H_6	4.659	1.924
H_o	0.693	0.943
H_m	0.329	0.220
H_p	0.261	0.132

Excellent agreement was obtained between the calculated induced shifts and the observed shifts for both of the conformers in a 34:66 (*exo*:*endo*) ratio at 25 °C obtained by the regression analysis between the observed and calculated data. Table 4 gives the observed and calculated ring current shifts in **12**. Again, excellent correlation of these data was obtained in a linear regression analysis [seven data points (range of the observed shift, 0.156–3.569 ppm) $\Delta\delta_{obs.} = a \bullet \Delta\delta_{calc.}$; a = 1.002, $R^2 = 0.9993$], with very small rms error (0.032 ppm).

Table 4. Observed (25 °C) and calculated ring current shifts of **12** (ppm)

Nucleus	Shifts	
	Obs.	Calc.
H_2	3.569	3.570
H_4	0.934	0.887
H_5	1.120	1.090
H_6	2.861	2.854
H_o	0.799	0.858
H_m	0.268	0.257
H_p	0.156	0.176

CONCLUSION

A new model of the porphyrin ring current effect has been presented based on a classical line current approximation. Satisfactory reproduction of the porphyrin induced-chemical-shift changes of ligands in several dicarboxylate Sn^{IV}(porphyrin) complexes was attained using only the newly developed ring current model. This clearly verified the validity of our assumption that the contribution of the complexation shift in the chemical shift changes of ligands is negligible in these complexes. In this ring current model, it is found that the current on the inner 16π-electron circuit is the main contributor and that on the outer 20π-electron circuit is the minor. The signs of the two contributors are opposite to each other indicating the opposite directions of the two currents. Theoretically, it is known that a 16π-electron ring current should be paratropic, hence, it is puzzling because all the protons of the ligands are high-field shifted and the observed shifts should be caused from the diatropic ring current. This issue can be explained clearly by considering all the possible circuit currents (p1–p4) of the porphyrin π-system. Since both of the 18-membered circuits (p2 and p3) are diatropic, summation of the two diatropic currents and the paratropic 20-membered circuit (p4) resulted in the net diatropic inner 16π-electron ring current of the porphyrin ring system. Using this ring current model, conformational analyses of bis(biphenylcarboxylate) complexes of Sn^{IV}(tpp) were carried out. From these analyses, it was found that the combination of the calculation of ligand shift values by using our porphyrin ring current model and DFT calculations is a useful technique for elucidating conformations of dicarboxylate Sn^{IV}(porphyrin) complexes in solution.

EXPERIMENTAL

General procedures

The ^{1}H NMR spectra were recorded with a JEOL-ECA 600, JEOL-Lambda 500 and Varian-Mercury 300 NMR spectrometer at 600, 500 and 300 MHz. All NMR experiments were obtained using the standard pulse programs and sequences.

General Method of NMR Experiment.

Tin porphyrin (0.003 mmol) was added to a solution of carboxylic acid (0.01 mmol) in $CDCl_3$ (1.0 ml). The mixture was sonicated at room temperature for 1 h. After 24 h, chemical shifts of dicarboxylate complex of Sn^{IV} porphyrin were measured.

ACKNOWLEDGEMENTS

This work was carried out with the support of the grant-in Aid for Scientific Research (No. 15350025) from the Ministry of Education, Science, Sports, and Culture, Japan, which is gratefully acknowledged.

REFERENCES

1. J. P. Collman, *Acc. Chem. Res.*, 1977, **10**, 265.
2. M. Momenteau and C. A. Reed, *Chem. Rev.*, 1994, **94**, 659.
3. M. J. Gunter and P. Turner, *Coord. Chem. Rev.* 1991, **108**, 115.
4. D. Holten, D. F. Bocian, and J. S. Lindsey, *Acc. Chem. Res.*, 2002, **35**, 57.
5. Y. Fukazawa, S. Usui, K. Tanimoto, and Y. Hirai, *J. Am. Chem. Soc.*, 1994, **116**, 8169.
6. T. Okajima, Z. H. Wang, and Y. Fukazawa, *Tetrahedron Lett.*, 1989, **30**, 1551.
7. T. Okajima, Z. H. Wang, and Y. Fukazawa, *Chem. Lett.*, 1991, 37.
8. Y. Fukazawa, K. Deyama, and S. Usui, *Tetrahedron Lett.*, 1992, **33**, 5803.
9. Z. H. Wang, S. Usui, and Y. Fukazawa, *Bull. Chem. Soc. Jpn.*, 1993, **66**, 1239.
10. Y. Fukazawa, T. Hayashibara, Y. Yang, and S. Usui, *Tetrahedron Lett.*, 1995, **36**, 3349.
11. Y. Fukazawa, Y. Yang, T. Hayashibara, and S. Usui, *Tetrahedron*, 1996, **52**, 2847.
12. H. Iwamoto, Y. Yang, S. Usui, and Y. Fukazawa, *Tetrahedron Lett.*, 2001, **42**, 49.

13. C. A. Hunter, C. M. R. Low, M. J. Packer, S. E. Spey, J. G. Vinter, M. O. Vysotsky, and C. Zonta, *Angew. Chem. Int. Ed.*, 2001, **40**, 2678.
14. R. J. Abraham, *Mol. Phys.*, 1961, **4**, 145.
15. R. J. Abraham, S. C. M. Fell, and K. M. Smith, *Org. Magn. Reson.*, 1977, **9**, 367.
16. R. J. Abraham, S. C. M. Fell, H. Pearson, and K. M. Smith, *Tetrahedron*, 1979, **35**, 1759.
17. R. J. Abraham, G. R. Bedford, D. McNeillie, and B. Wright, *Org. Magn. Reson.*, 1980, **14**, 418.
18. R. J. Abraham, *J. Mag. Res.*, 1981, **43**, 491.
19. R. J. Abraham, K. M. Smith, D. A. Goff, and J. J. Lai, *J. Am. Chem. Soc.*, 1982, **104**, 4332.
20. R. J. Abraham and K. M. Smith, *J. Am. Chem. Soc.*, 1983, **105**, 5734.
21. K. M. Smith, F. W. Bobe, O. M. Minnetian, and R. J. Abraham, *Tetrahedron*, 1984, **40**, 3263.
22. K. M. Smith, F. W. Bobe, D. A. Goff, and R. J. Abraham, *J. Am. Chem. Soc.*, 1986, **108**, 1111.
23. R. J. Abraham, C. J. Medforth, K. E. Mansfield, D. J. Simpson, and K. M. Smith, *J. Chem. Soc., Perkin Trans. 2*, 1988, 1365.
24. R. J. Abraham, A. E. Rowan, D. A. Goff, K. E. Mansfield, and K. M. Smith, *J. Chem. Soc., Perkin Trans. 2*, 1989, 1633.
25. R. J. Abraham and I. Marsden, *Tetrahedron*, 1992, **48**, 7489.
26. C. J. Medforth, C. M. Muzzi, K. M. Shea, K. M. Smith, R. J. Abraham, S. Jia, and J. A. Shelnutt, *J. Chem. Soc., Perkin Trans. 2*, 1997, 839.
27. J. S. Waugh and R. W. Fessenden, *J. Am. Chem. Soc.*, 1957, **79**, 846.
28. C. E. Johnson, Jr. and F. A. Bovey, *J. Chem. Phys.*, 1958, **29**, 1012.
29. S. J. Perkins, *J. Mag. Res.*, 1980, **38**, 297.
30. C. W. Haigh and R. B. Mallion, *Mol. Phys.*, 1971, **22**, 955.
31. R. M. Gomila, D. Quinonero, C. Rotger, C. Garau, A. Frontera, P. Ballester, A. Costa, and P. M. Deya, *Org. Lett.*, 2002, **4**, 399.
32. J. Juselius and D. Sundholm, *Phys. Chem. Chem. Phys.*, 2000, **2**, 2145.
33. J. Juselius and D. Sundholm, *J. Org. Chem.*, 2000, **65**, 5233.
34. E. Steiner and P. W. Fowler, *ChemPhysChem*, 2002, **3**, 114.
35. E. D. Becker and R. B. Bradley, *J. Chem. Phys.*, 1959, **31**, 1413.
36. C. J. Medforth, *Porphyrin Handbook*, 2000, **5**, 1.
37. H. Iwamoto, K. Hori, and Y. Fukazawa, *Tetrahedron Lett.*, 2005, **46**, 731.
38. H. Iwamoto and Y. Fukazawa, *Heterocycles*, 2005, **65**, 523.
39. H. Iwamoto, K. Hori, and Y. Fukazawa, *Tetrahedron*, 2006, **62**, 2789.
40. H. C. Longuet-Higgins and L. Salem, *Proc. Roy. Soc. (London)*, 1960, **A257**, 445.
41. Gaussian 03, Revision C.02, M. J. Frisch, G. W. Trucks, H. B. Schlegel, G. E. Scuseria, M. A. Robb,

J. R. Cheeseman, J. A. Montgomery, Jr., T. Vreven, K. N. Kudin, J. C. Burant, J. M. Millam, S. S. Iyengar, J. Tomasi, V. Barone, B. Mennucci, M. Cossi, G. Scalmani, N. Rega, G. A. Petersson, H. Nakatsuji, M. Hada, M. Ehara, K. Toyota, R. Fukuda, J. Hasegawa, M. Ishida, T. Nakajima, Y. Honda, O. Kitao, H. Nakai, M. Klene, X. Li, J. E. Knox, H. P. Hratchian, J. B. Cross, V. Bakken, C. Adamo, J. Jaramillo, R. Gomperts, R. E. Stratmann, O. Yazyev, A. J. Austin, R. Cammi, C. Pomelli, J. W. Ochterski, P. Y. Ayala, K. Morokuma, G. A. Voth, P. Salvador, J. J. Dannenberg, V. G. Zakrzewski, S. Dapprich, A. D. Daniels, M. C. Strain, O. Farkas, D. K. Malick, A. D. Rabuck, K. Raghavachari, J. B. Foresman, J. V. Ortiz, Q. Cui, A. G. Baboul, S. Clifford, J. Cioslowski, B. B. Stefanov, G. Liu, A. Liashenko, P. Piskorz, I. Komaromi, R. L. Martin, D. J. Fox, T. Keith, M. A. Al-Laham, C. Y. Peng, A. Nanayakkara, M. Challacombe, P. M. W. Gill, B. Johnson, W. Chen, M. W. Wong, C. Gonzalez, and J. A. Pople, Gaussian, Inc., Wallingford CT, 2004.

42. R. J. Abraham and C. J. Medforth, *Magn. Reson. Chem.*, 1987, **25**, 432.
43. Y. Fukazawa, K. Ogata, and S. Usui, *J. Am. Chem. Soc.*, 1988, **110**, 8692.
44. B. A. Hess, Jr., L. J. Schaad, and M. Nakagawa, *J. Org. Chem.*, 1977, **42**, 1669.
45. K. Müllen, T. Meul, P. Schade, H. Schmickler, and E. Vogel, *J. Am. Chem. Soc.*, 1987, **109**, 4992.
46. K. Müllen, W. Huber, T. Meul, M. Nakagawa, and M. Iyoda, *J. Am. Chem. Soc.*, 1982, **104**, 5403.
47. J. Aihara, *Bull. Chem. Soc. Jpn.*, 2004, **77**, 651.